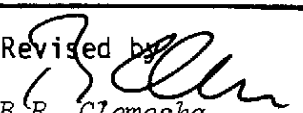

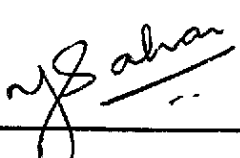


1. Classification <i>INPE.COM 4(RPE)</i> <i>CDU:523.4-853</i>		2. Period <i>September/80</i>	4. Distribution Criterion  internal <input type="checkbox"/> external <input checked="" type="checkbox"/>
3. Key Words (selected by the author) <i>OI 7774 Å</i> <i>[OI] 6300 Å</i> <i>IONOSPHERIC PARAMETERS</i>			
5. Report No. <i>INPE-1911-RPE/244</i>	6. Date <i>September 1980</i>	7. Revised by  <i>B.R. Clemesha</i>	
8. Title and Sub-title <i>SIMULTANEOUS OBSERVATIONS OF OI 7774 Å AND [OI] 6300 Å EMISSIONS AND CORRELATIVE STUDY WITH IONOSPHERIC PARAMETERS</i>		9. Authorized by  <i>Nelson de Jesus Parada</i> <i>Director</i>	
10. Sector <i>DGA/DOA</i>	Code <i>30.313</i>	11. No. of Copies <i>09</i>	
12. Authorship <i>Y. Sahai</i> <i>J.A. Bittencourt</i> <i>N.R. Teixeira</i> <i>H. Takahashi</i>		14. No. of Pages <i>18</i>	
13. Signature of first author 		15. Price	
16. Summary/Notes  <i>Regular measurements of the OI 7774 Å and [OI] 6300 Å nightglow emissions were carried out at Cachoeira Paulista (22.7°S, 45.0°W), Brazil, during the period of April 1978 to March 1979. An ionosonde is also operated at Cachoeira Paulista. A correlative study of the OI 7774 Å and [OI] 6300 Å emission observations, with simultaneous ionosonde measurements, shows good correlations between <math>(J_{7774})^{1/2}</math> and F-layer peak electron density <math>(n_m(e))</math>, and between the ratio <math>(J_{7774})^{1/2} / (J_{6300})</math> and the height of the F-layer (<math>h_m F_2</math>), where <math>J_{7774}</math> and <math>J_{6300}</math> are the column emission rates for the OI 7774 Å and [OI] 6300 Å emissions respectively. Simultaneous measurements of these two emissions would be a very useful technique for remote sensing of the ionospheric F-layer dynamics.</i>			
17. Remarks <i>"This work was partially supported by the Brazilian National Fund for Science and Technology under contract FINEP-537/CT".</i>			

INDEX

1. INTRODUCTION .....	1
2. THEORY .....	2
3. INSTRUMENTATION .....	4
4. OBSERVATIONS AND DISCUSSION .....	4
5. CONCLUSIONS .....	5
6. ACKNOWLEDGEMENTS .....	6
REFERENCES .....	7

SIMULTANEOUS OBSERVATIONS OF OI 7774 Å AND [OI] 6300 Å EMISSIONS  
AND CORRELATIVE STUDY WITH IONOSPHERIC PARAMETERS

Y.Sahai, J.A.Bittencourt, N.R.Teixeira and H. Takahashi

Instituto de Pesquisas Espaciais - INPE  
Conselho Nacional de Desenvolvimento Científico e Tecnológico - CNPq  
12.200 - São José dos Campos, São Paulo, Brazil

ABSTRACT

Regular measurements of the OI 7774 Å and [OI] 6300 Å nightglow emissions were carried out at Cachoeira Paulista (22.7°S, 45.0°W), Brazil, during the period of April 1978 to March 1979. An ionosonde is also operated at Cachoeira Paulista. A correlative study of the OI 7774 Å and [OI] 6300 Å emission observations, with simultaneous ionosonde measurements, shows good correlations between  $(J_{7774})^{1/2}$  and F-layer peak electron density ( $n_m(e)$ ), and between the ratio  $(J_{7774})^{1/2} / (J_{6300})$  and the height of the F-layer ( $h_m F_2$ ), where  $J_{7774}$  and  $J_{6300}$  are the column emissions rates for the OI 7774 Å and [OI] 6300 Å emissions, respectively. Simultaneous measurements of these two emissions would be a very useful technique for remote sensing of the ionospheric F-layer dynamics.

SIMULTANEOUS OBSERVATIONS OF OI 7774 Å AND [OI] 6300 Å EMISSIONS  
AND CORRELATIVE STUDY WITH IONOSPHERIC PARAMETERS

Y.Sahai, J.A.Bittencourt, N.R.Teixeira and H. Takahashi

Instituto de Pesquisas Espaciais - INPE  
Conselho Nacional de Desenvolvimento Científico e Tecnológico - CNPq  
12.200 - São José dos Campos, São Paulo, Brazil

1. INTRODUCTION

Tinsley and Bittencourt (1975) and Chandra et al. (1975) investigated the possibility of using airglow observations for determination of the F-region height and peak electron density. Tinsley and Bittencourt (1975) considered the OI 1356 Å (radiative recombination with a small contribution from ion-ion recombination) and [OI] 6300 Å (dissociative recombination) emissions and showed that, if  $J_{1356}$  and  $J_{6300}$  are vertical column emissions rates, to a very good approximation, the peak electron density,  $n_m(e)$  is proportional to  $(J_{1356})^{1/2}$  and, to a good approximation, the ratio  $(J_{1356})^{1/2} / J_{6300}$  is a single-valued function of the layer height,  $h_m F_2$ .

During the period of April 1978 - March 1979, simultaneous measurements of the OI 7774 Å and [OI] 6300 Å emissions were carried out at Cachoeira Paulista (22.7°S, 45.0°W), Brazil, where an ionosonde was also operating. The major source for the tropical OI 7774 Å emission is also radiative recombination (Tinsley et al., 1973). Therefore, an experimental correlative study of the F-region parameters obtained by airglow observations, as suggested by Tinsley and Bittencourt (1975), and by simultaneous ionosonde measurements was carried out. The results are presented and discussed in this paper.

## 2. THEORY

Tinsley et al. (1973) have discussed in detail the excitation of oxygen permitted line emissions in the tropical nightglow, and concluded that radiative recombination is the major source for the OI 7774 emission, with a small contribution from ion-ion recombination. Using the same formalism and notation as that of Tinsley and Bittencourt (1975), the column emission rate,  $J_{7774}$ , is given by

$$J_{7774} = n_m^2(e) \int \alpha_{7774} s^2(z) dz + n_m^2(e) \int \frac{\beta_{7774} K_1 K_2 n(0) s^2(z) dz}{K_2 n_m(e) s(z) + K_3 n(0)} \quad (1)$$

from their equation (11), replacing the OI 1356 emission by the OI 7774 emission, where  $\alpha_{7774}$  is the partial rate coefficient for radiative recombination;  $\beta_{7774}$  is the fraction of the total ion-ion recombination yielding the transition 7774;  $n_m(e)$  is the electron density at the F - layer peak and  $S(z)$  is a shape factor for the F - layer [ $n(e) = n_m(e) S(z)$ ];  $n(0)$  is the atomic oxygen density;  $K_1$ ,  $K_2$ , and  $K_3$  are reaction rate coefficients; and  $z$  denotes the height.

For the [OI] 6300 emission, the column emission rate,  $J_{6300}$ , due to dissociative recombination, is given by (see equation (9) of Tinsley and Bittencourt, 1975)

$$J_{6300} = K A_{6300} n_m(e) \int \frac{\gamma_1 n(O_2) s(z) dz}{A [1 + d(z) / A] [1 + B(z)]} \quad (2)$$

where  $K$  is the quantum efficiency (i.e., the fraction of  $O(^1D)$  states produced per dissociative recombination of  $O_2^+$ );  $A$  and  $A_{6300}$  denote the Einstein Coefficients for transition from the  $^1D$  state and for the transition leading to the 6300 Å emission, respectively;  $\gamma_1$  is the reaction rate coefficient for the dissociative recombination of  $O_2^+$ ;

$n(O_2)$  is the molecular oxygen density;  $d(z)$  is the height dependent quenching frequency; and  $B(z)$  is a combination of rate coefficients and particle concentrations, and is important only below about 200 km (Peterson and VanZandt, 1969).

Figures 1 and 2 show the calculated variations of  $(J_{7774})^{1/2}$  with  $n_m(e)$  for different F-layer peak heights, and the ratio  $(J_{7774})^{1/2} / (J_{6300})$  against  $h_m F_2$ , for different F-layer peak electron densities, respectively. The numerical integration using equations (1) and (2) were carried out over the range 150-800 km and the F-layer shape,  $S(z)$ , was assumed to be a modified Chapman function (Tinsley and Bittencourt, 1975). Exospheric temperatures and density profiles were calculated using Walker's (1965) analytical form of Jacchia (1965). The coefficients used were:  $\alpha_{7774} = 5.8 \times 10^{-13} \text{ cm}^3 \text{ sec}^{-1}$  (Tinsley et al., 1973);  $\beta_{7774} = 0.42$  (Olsen et al., 1971);  $K_1 = 1.3 \times 10^{-15} \text{ cm}^3 \text{ sec}^{-1}$  (Massey, 1969);  $K_2 = 1.0 \times 10^{-7} \text{ cm}^3 \text{ sec}^{-1}$  (Olsen et al., 1971);  $K_3 = 1.4 \times 10^{-10} \text{ cm}^3 \text{ sec}^{-1}$  (Fehsenfeld et al., 1969);  $\gamma_1 = 2.0 \times 10^{-11} (300/T) \text{ cm}^3 \text{ sec}^{-1}$  (Donahue, 1968);  $\gamma_2 = 1.0 \times 10^{-12} (300/T) \text{ cm}^3 \text{ sec}^{-1}$  (Donahue, 1968);  $\alpha_1 = 1.0 \times 10^{-7} (700/T) \text{ cm}^3 \text{ sec}^{-1}$  (Biondi, 1969);  $\alpha_2 = 2.0 \times 10^{-7} (700/T) \text{ cm}^3 \text{ sec}^{-1}$  (Biondi, 1969), ( $\gamma_2$ ,  $\alpha_1$  and  $\alpha_2$  were used to calculate  $B(z)$ );  $SN_2 = 7.0 \times 10^{-11} \text{ cm}^3 \text{ sec}^{-1}$  (Forbes, 1970) and  $S_e = 1.7 \times 10^{-9} \text{ cm}^3 \text{ sec}^{-1}$  (Seaton, 1955), ( $SN_2$  and  $S_e$  are quenching coefficients to calculate  $d(z)$ );  $A_{6300} = 0.0069 \text{ sec}^{-1}$ ;  $A = 0.0091 \text{ sec}^{-1}$ ;  $K = 1.0$ .

It is observed, from Figure 1, that the dependence of  $(J_{7774})^{1/2}$  on  $n_m(e)$  is little affected by exospheric temperature and F-layer peak height. Figure 2 shows that the dependence of the ratio  $(J_{7774})^{1/2} / (J_{6300})$  on  $h_m F_2$  is strongly affected by exospheric temperature changes, while the influence of the peak electron density is small.

### 3. INSTRUMENTATION

Both the emissions were observed with tilting filter-type photometers looking in the zenith direction. The 7774 photometer has an aperture of 65 mm with a field of view of  $3^\circ$  full angle (Sahai et al., 1980) and scan time of 150 secs. The 6300 photometer has an aperture of 50 mm with a field of view of  $5^\circ$  full angle. The interference filter (bandwidth  $\sim 11 \text{ \AA}$ ) alternates between two positions to give the on-line and background intensities (Sahai et al., 1974). The ionospheric parameters, used for the study, were obtained from an ionosonde (Magnetic AB model 10005W) operating at a nearby location.

### 4. OBSERVATIONS AND DISCUSSION

In order to compare the F-region parameters, obtained by the airglow emissions and ionosonde, data for three nights were selected, viz. May 3-4, September 25-26 and October 2-3, 1978. On these nights, observations for both the emissions were available for almost the complete night, and ionograms showed very small or no spread-F, thereby permitting a better estimate of the F-region heights ( $h_p F_2$ ) and peak electron densities ( $n_m(e)$ ) for comparison.

Figures 3 and 4 show the local time variations of the observed  $(J_{7774})^{1/2}$  and  $n_m(e)$ , and the ratio  $(J_{7774})^{1/2} / (J_{6300})$  and  $h_p F_2$ , respectively. It may be noted, from these figures, that there is a good correlation between the time variations of  $(J_{7774})^{1/2}$  and  $n_m(e)$ , and the ratio  $(J_{7774})^{1/2} / (J_{6300})$  and  $h_p F_2$ . The observed  $(J_{7774})^{1/2}$  and  $n_m(e)$ , and the ratio  $(J_{7774})^{1/2} / (J_{6300})$  and  $h_p F_2$  are also shown (as dots) in Figures 1 and 2, respectively, and the variations exhibit similar characteristics to those obtained from theoretical calculations. The large scatter of points in Figure 2 is considered to be due to exospheric temperature changes during the course of night and from one night to another, since data from different nights have been plotted together

Figure 5 shows a plot of  $n_m(e)$  from the ionosonde against  $n_m(e)$  - airglow, obtained from the observed  $J_{7774}$  and using the calculated variation of the  $(J_{7774})^{1/2}$  with  $n_m(e)$  shown in Figure 1. Second order dependences on the F-layer heights and exospheric temperatures were neglected. The plot should correspond to a ratio of unity and fall on a straight line of  $45^\circ$  slope. The plot shows a linear variation but the best-fit line (dashed) shows a slight departure from the  $45^\circ$  slope which could be due to calibration errors in the airglow measurements or departures from the Chapman Layer shape (Tinsley and Bittencourt, 1975) and other assumptions inherent to the numerical calculation. In any case, the linear relationship between  $n_m(e)$  - ionosonde and  $n_m(e)$  - airglow indicates the usefulness of the OI 7774 Å measurements to estimate the F-layer peak density.

Figure 6 shows a plot of the  $h_p F_2$  - ionosonde and  $h_m F_2$  - airglow, obtained from Figure 2 using the observed  $J_{7774}$  and  $J_{6300}$ . The exospheric temperatures for these nights were calculated using Jacchia (1971) to determine  $h_m F_2$  - airglow, but second order dependence on  $n_m(e)$  was neglected. Here, also, the best-fit line (dashed) of the plot departs from a  $45^\circ$  slope, showing a rather systematic departure. Again, the departure could be due to calibration errors in airglow measurements or assumptions in the numerical calculations. But, again, the near linear variation of  $h_m F_2$  - airglow with  $h_p F_2$  - ionosonde indicates the usefulness of simultaneous measurements of the [OI] 6300 Å and OI 7774 Å emissions to estimate the F-layer peak height.

## 5. CONCLUSIONS

A correlative study of the OI 7774 Å and [OI] 6300 Å emission observations with simultaneous ionosonde measurements of ionospheric F-region parameters shows good correlations between  $(J_{7774})^{1/2}$  and  $n_m(e)$ , and between the ratio  $(J_{7774})^{1/2} / (J_{6300})$  and  $h_m F_2$ . It is, therefore, observed that the information obtained by simultaneous ground-based observations of the OI 7774 Å and



[OI] 6300 Å emissions can be converted to F-region peak heights and densities, producing, in some respects, results equivalent to those from an ionosonde. However, the technique is not limited to vertical sounding. Photometers to measure these emissions with all-sky scanning capability could provide a map of the whole sky for the study of the F-region, and, in particular, propagation of ionospheric disturbances and waves. An ionosonde within the region covered by the photometers could provide a calibration point where the ionosonde beam is located. It should be pointed out that the method described here works best at low latitudes where usually the electron densities are high at night.

#### 6. ACKNOWLEDGEMENTS

We thank B.A. Tinsley for helpful discussions and M.A. Abdu for ionospheric data. This work was partially supported by the Brazilian National Fund for Science and Technology under contract FINEP-537/CT.

FIGURE CAPTIONS

- Fig. 1 - Variation of  $(J_{7774})^{1/2}$  with  $n_m(e)$  for exospheric temperatures of  $1200^{\circ}\text{K}$  and  $800^{\circ}\text{K}$  and F-layer peak heights of 250 and 390 km. Dots are the plots of the observed  $(J_{7774})^{1/2}$  against  $n_m(e)$  from the ionosonde.
- Fig. 2 - Variation of the ratio  $(J_{7774})^{1/2} / (J_{6300})$  with  $h_m F_2$  for exospheric temperatures of  $1200^{\circ}\text{K}$ ,  $1000^{\circ}\text{K}$  and  $800^{\circ}\text{K}$  and peak electron densities  $1 \times 10^5$ ,  $5 \times 10^5$  and  $5 \times 10^6 \text{ cm}^{-3}$ . Dots are the plots of the observed ratios  $(J_{7774})^{1/2} / (J_{6300})$  against  $h_p F_2$  from the ionosonde.
- Fig. 3 - Local time variations of the observed  $(J_{7774})^{1/2}$  and  $n_m(e)$  from the ionosonde for May 3-4, September 25-26 and October 2-3, 1978.
- Fig. 4 - Local time variations of the observed ratio  $(J_{7774})^{1/2} / (J_{6300})$  and  $h_p F_2$  from the ionosonde for May 3-4, September 25-26 and October 2-3, 1978.
- Fig. 5 - Plot of  $n_m(e)$  - ionosonde against  $n_m(e)$  - airglow obtained from the observed  $J_{7774}$  and using calculated variations of  $(J_{7774})^{1/2}$  and  $n_m(e)$  given in Figure 1.
- Fig. 6 - Plot of  $h_p F_2$  - ionosonde against  $h_m F_2$  - airglow obtained from the observed  $J_{7774}$  and  $J_{6300}$ , and using calculated variation of  $(J_{7774})^{1/2} / (J_{6300})$  and  $h_m F_2$  given in Figure 2.

REFERENCES

- Biondi, M.A. Atmospheric electron-ion and ion-ion recombination processes, *Can. J. Chem.*, 47, 1711-1719, 1969.
- Chandra, S., E.I. Reed, R.R. Meier, C.B. Opal and G.T. Hicks, Remote Sensing of the ionospheric F layer using airglow techniques, *J. Geophys. Res.*, 80, 2327-2332, 1975.
- Donahue, T.M. Ionospheric composition and reactions, *Science*, 159, 489-498, 1968.
- Fehsenfeld, F.A., A.C. Schmeltekopf, D.B. Dunkin and E.E. Ferguson, Compilation of reaction rate constants measured in the ESSA flowing afterglow system, Tech. Rep. ERL 135-AL3, ESSA, Boulder, Colo., 1969.
- Forbes, J.M. Yield of  $O(^1D)$  by dissociative recombination of  $O_2^+$  from night airglow observations, *J. Atmos. Terr. Phys.*, 32, 1901-1908, 1970.
- Jacchia, L.G. Static diffusion models of the upper atmosphere with empirical temperature profiles, *Smithson. Contrib. Astrophys.*, 8, 215, 1965.
- Jacchia, L.G. Revised static models of the thermosphere and exosphere with empirical temperature profiles, Smithsonian Astrophysical Observatory, Special report 332, May 1971.
- Massey, H.S.W. Electronic and ionic impact phenomena, vol.2, p.1265. Clarendon Press, London, 1969.
- Olsen, R.E., J.R. Peterson and J. Moseley, Oxygen ion-ion neutralization reaction as related to tropical ultraviolet nightglow, *J. Geophys. Res.*, 76, 2516-2519, 1971.
- Peterson, V.L., and T.E. VanZandt,  $O(^1D)$  quenching in the ionospheric F-region, *Planet. Space Sci.*, 17, 1725, 1969.

- Sahai, Y., N.R. Teixeira, P.D. Angreji, J.A. Bittencourt and H. Takahashi, Tropical F-region nightglow enhancements in the Brazilian sector, *Ann. Geophys.*, 30, 397-403, 1974.
- Sahai, Y., J.A. Bittencourt, N.R. Teixeira and H. Takahashi, Plasma irregularities in the tropical F-region detected by OI 7774 Å and 6300 Å nightglow measurements, submitted to *J. Geophys. Res.*, 1980.
- Seaton, M.J. The calculation of cross-sections for excitations of forbidden atomic lines by electron impact, *J. Atmos. Terr. Phys.*, 5, 289, 1955.
- Tinsley, B.A., A.B. Cristensen, J. Bittencourt, H. Gouveia, P.D. Angreji, and H. Takahashi, Excitation of oxygen permitted line emissions in the tropical nightglow, *J. Geophys. Res.*, 78, 1174-1186, 1973.
- Tinsley, B.A. and J.A. Bittencourt, Determination of F-region height and peak electron density at night using airglow emissions from atomic oxygen, *J. Geophys. Res.*, 80, 2333-2337, 1975.
- Walker, J.C.G. Analytical representation of upper atmosphere densities based on Jacchia's static diffusion models, *J. Atmos. Sci.*, 22, 462-463, 1965.

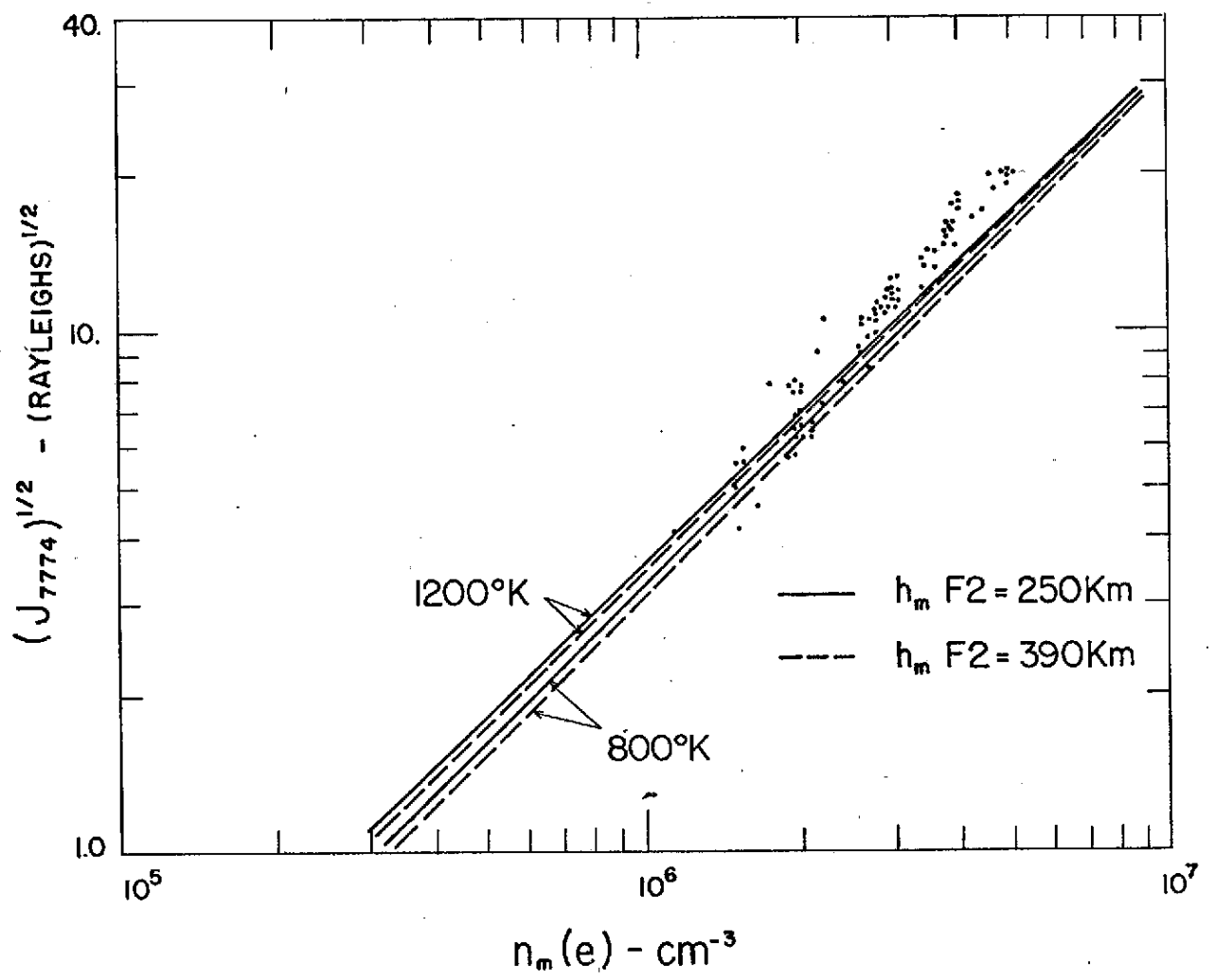


Figure 1

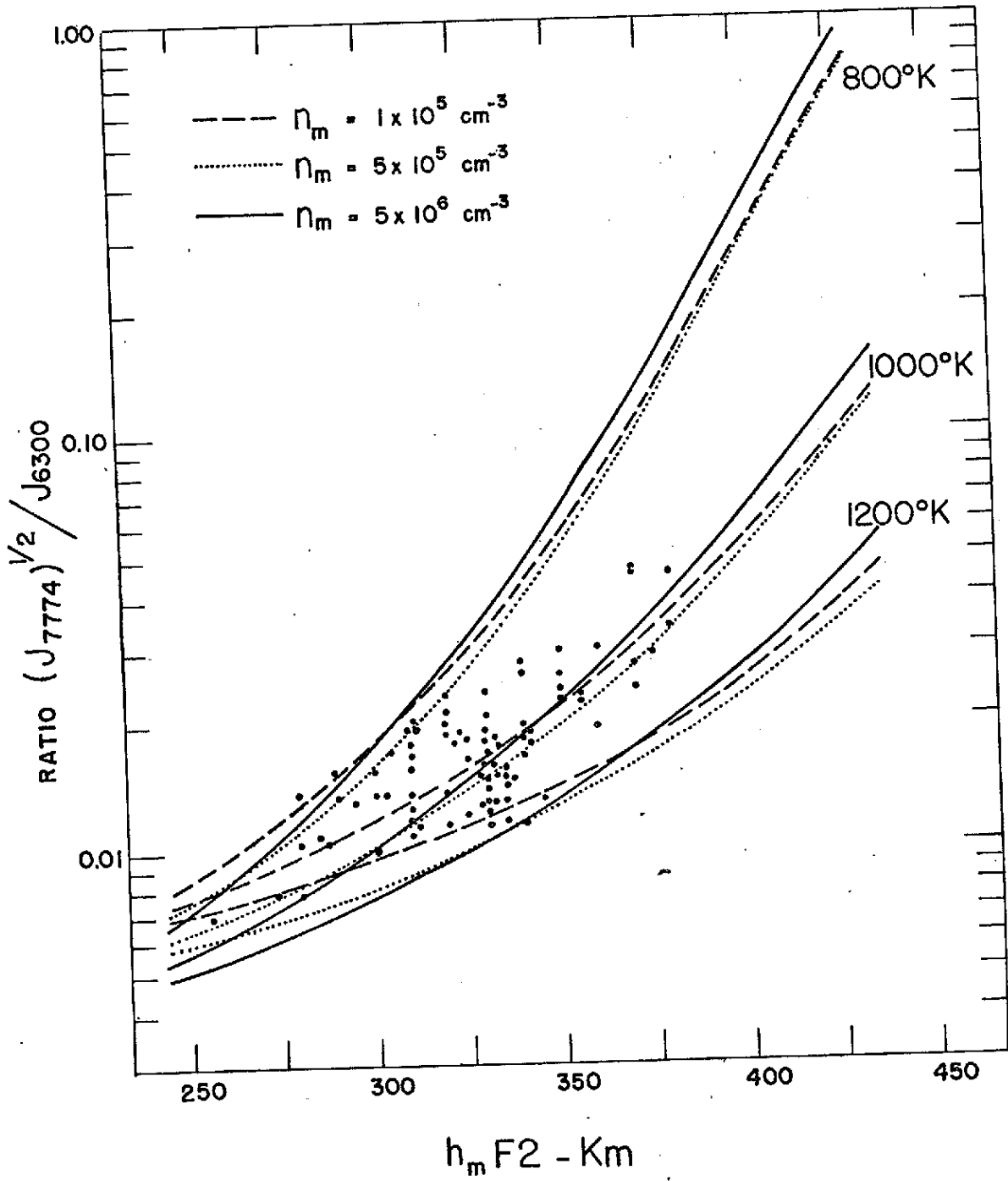


Figure 2

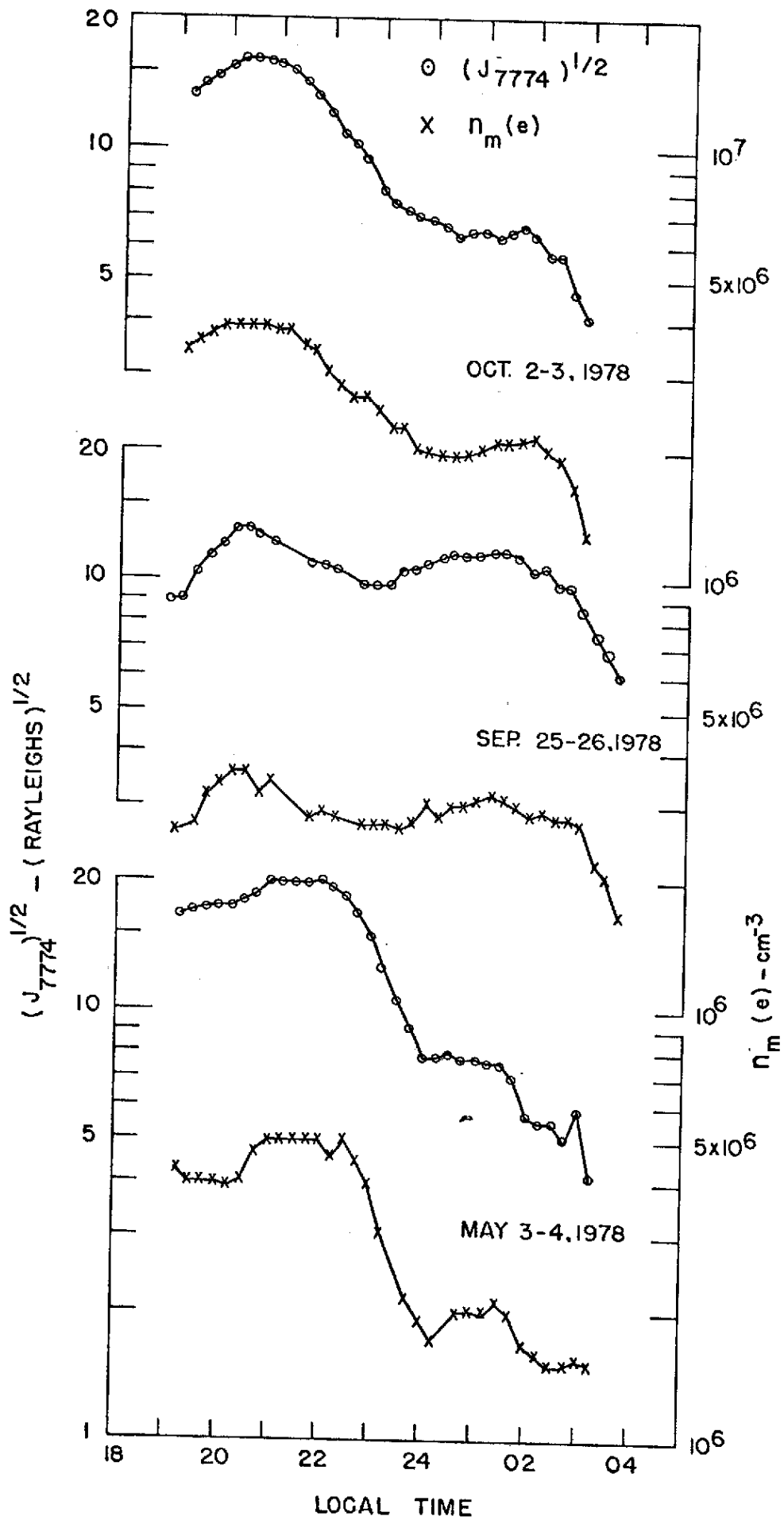


Figure 3

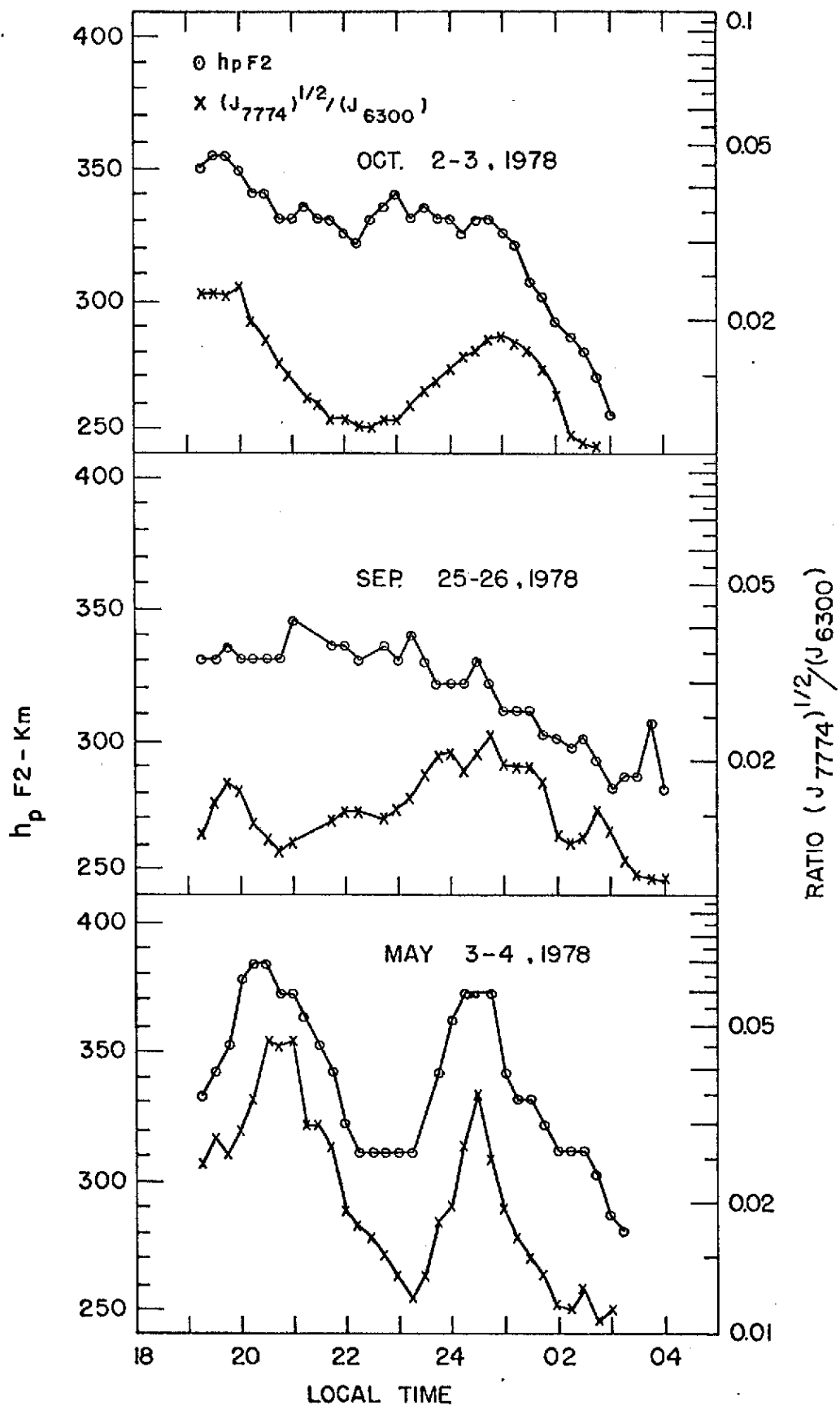


Figure 4



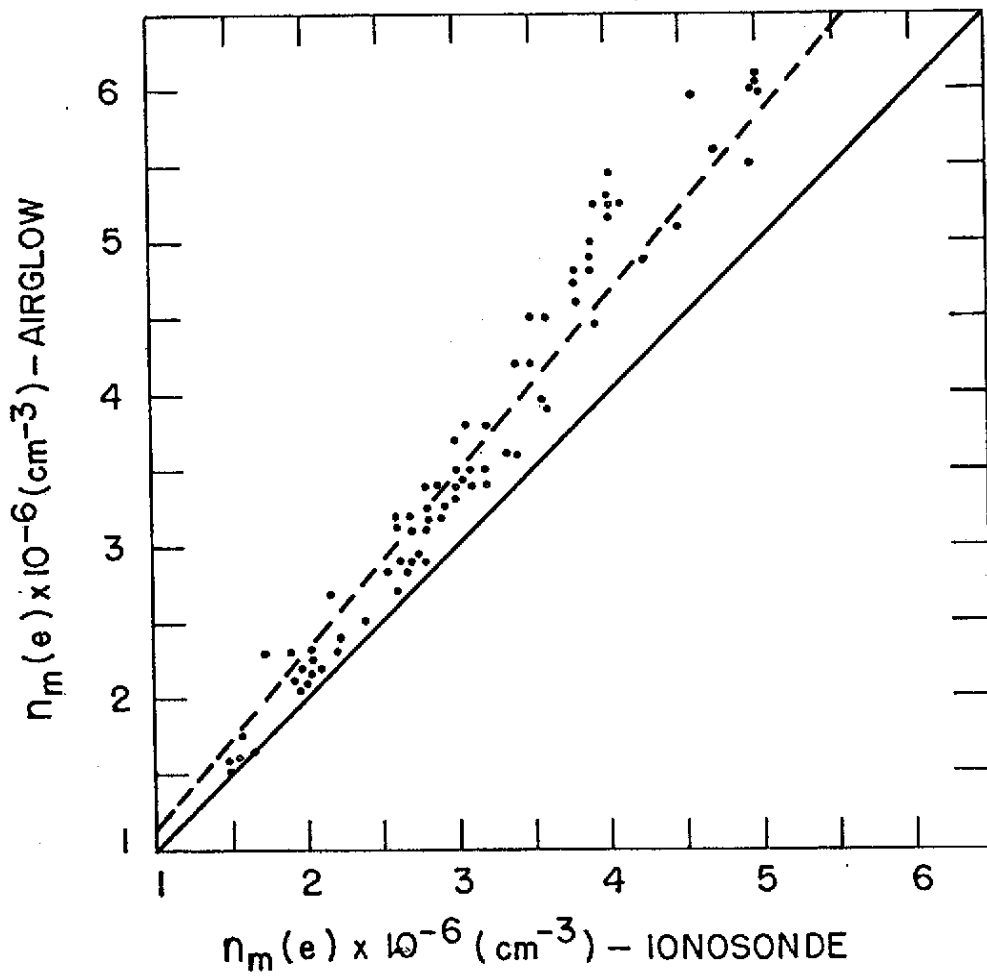


Figure 5

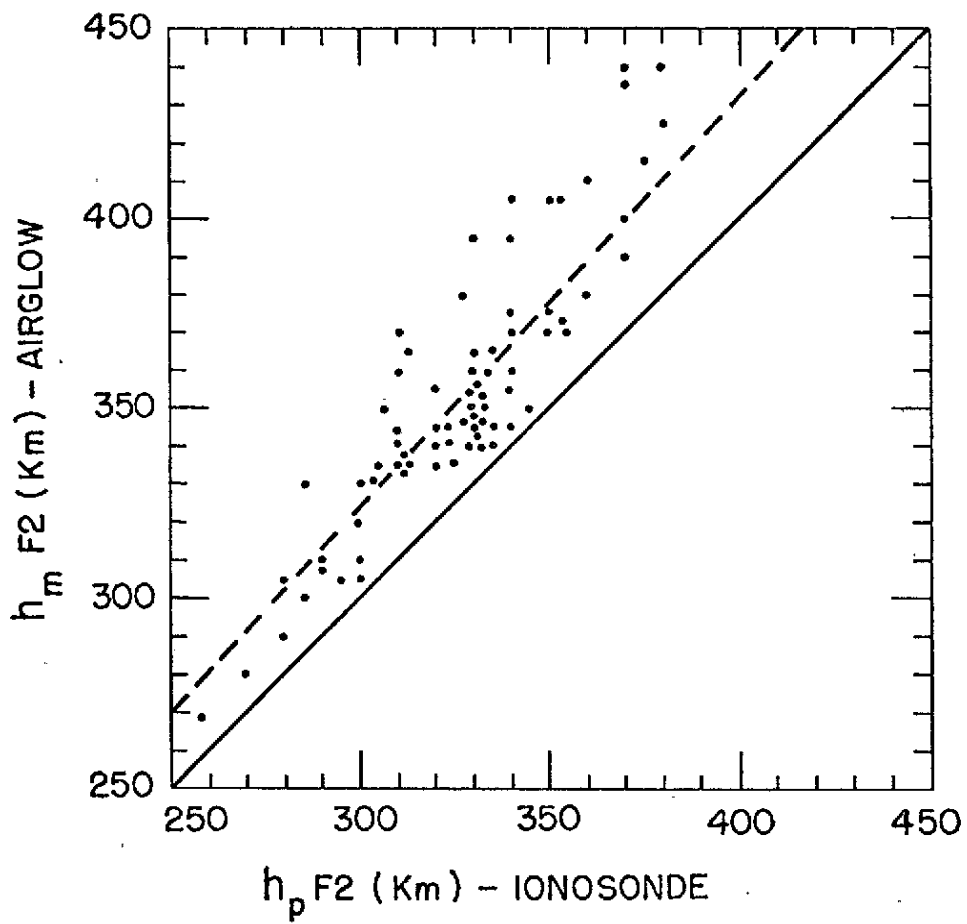


Figure 6